AD-A070 596 MARYLAND UNIV COLLEGE PARK DEPT OF PHYSICS AND ASTRONOMY F/G 7/4
THE INFLUENCE OF AUTOIONIZATION ACCOMPANIED BY EXCITATION ON TH--ETC(U)
OCT 76 V L JACOBS, J DAVIS, P C KEPPLE N00014-75-C-0309

UNCLASSIFIED NL

1 OF 1
AD
A070596

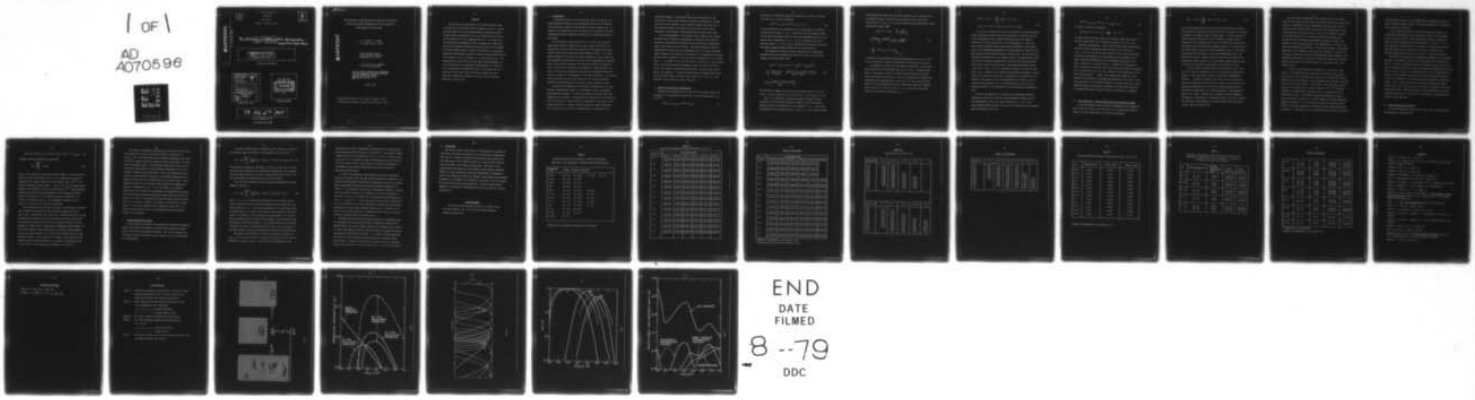

END
DATE
FILMED
8-79
DDC

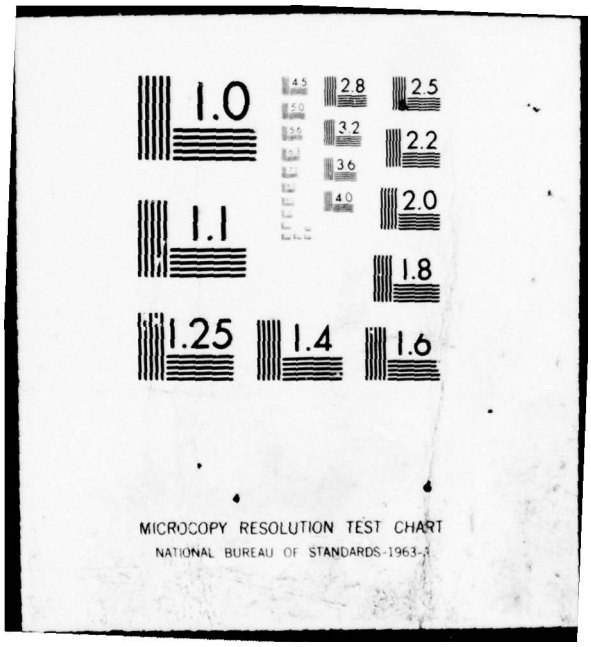
1.0
1.1
1.25
1.4
1.6
1.8
2.0
2.2
2.5
2.8
3.2
3.6
4.0
4.5
5.0
5.6
MICROCOPY RESOLUTION TEST CHART
NATIONAL BUREAU OF STANDARDS-1963-A

DDC PROCESSING DATA

PHOTOGRAPH THIS SHEET

RETURN TO DDA-2 FOR FILE

II
LEVEL

1
INVENTORY

AD A070596

DDC ACCESSION NUMBER

The Influence of Autoionization Accompanied by---

DOCUMENT IDENTIFICATION Jacobs, Davis, Kepple and Blaha

DISTRIBUTION STATEMENT A
Approved for public release;
Distribution Unlimited

DISTRIBUTION STATEMENT

Accession For
NTIS GRA&I X
DDC TAB
Unannounced
Justification
By
Distribution/
Availability Codes
Dist. | Avail and/or special
A

DISTRIBUTION STAMP

DDC
RECEIVED
JUN 29 1979
D

DATE ACCESSIONED

79 06 27 307

DATE RECEIVED IN DDC

PHOTOGRAPH THIS SHEET

THE INFLUENCE OF AUTOIONIZATION ACCOMPANIED BY EXCITATION ON THE DIELECTRONIC RECOMBINATION AND THE IONIZATION EQUILIBRIUM OF SILICON IONS

V. L. Jacobs†, J. Davis,
P. C. Kepple and M. Blaha*

Plasma Dynamics Branch
Naval Research Laboratory
Washington, D.C. 20375

Work on this report was supported by ONR Contract N00014-75-C-0309 and/or N00014-67-A-0239 monitored by NRL 6702.02.

October 1976

†Science Applications, Inc., McLean, Virginia 22101

*University of Maryland, College Park, Maryland 20742

Abstract

The dielectronic recombination rate coefficients have been calculated for the various ionization stages of silicon. Account has been taken of all stabilizing radiative transitions and all autoionization processes which involve a single-electron electric-dipole transition of the recombining ion core. For certain ions the dielectronic recombination rates, although still larger than the direct radiative recombination rates, are found to be substantially reduced when account is taken of the effects of a previously neglected autoionization process in which the excited recombining ion core undergoes a $\Delta n = 0$ transition to a lower excited state. The temperatures at which these ions have their maximum abundance in corona equilibrium are significantly reduced when use is made of the new dielectronic recombination rates. Calculations are also presented for the total rates of radiative energy loss from isothermal steady-state plasmas due to the line and continuum emission of silicon ions.

I. Introduction

An important method of investigating the physical properties of high-temperature laboratory and astrophysical plasmas is the analysis of optically-thin spectral lines emitted by multiply-charged ions. In addition, the energy loss due to the emitted far ultraviolet and x-ray radiation may have a significant influence on the dynamical behavior of the plasma.

At low densities, where practically all excited ions cascade to their ground states in times that are short compared with the total electron-ion collision time, the spectral line intensities can be predicted on the basis of the corona model (McWhirter 1965). The steady-state abundance of the various ionization stages of a given element can be determined as functions of the local electron temperature by assuming that electron impact ionization from the ground states is balanced by direct radiative and dielectronic recombination. Photoionization and stimulated radiative recombination processes are neglected because the plasma is assumed to be transparent to the emitted radiation. The spectral line intensities can then be calculated from the corona ionization equilibrium distributions and the electron impact excitation rates.

Dielectronic recombination has been shown (Burgess 1964) to be the dominant recombination process for nonhydrogenic ions in low-density high-temperature plasmas. In addition, Gabriel and Jordan (1972) have emphasized the importance of determining the contribution to the resonance line intensity due to spectroscopically unresolvable dielectronic recombination satellites. Burgess (1965) has obtained a simple expression for estimating the dielectronic recombination rate coefficients for

low-density plasmas. The Burgess formula has been employed in the calculation of the corona ionization equilibrium distriubtions (Jordan 1969) and in the evaluation of the radiative energy loss rates due to collisionally-induced line emission (Cox and Tucker 1969), and the importance of dielectronic recombination has been firmly established.

In this investigation a more general theory (Jacobs, Davis, Kepple, and Blaha 1977), referred to subsequently as JDKB, has been applied in systematic and detailed calculations for the dielectronic recombination rates of the various ions of silicon. The Burgess formula is found to overestimate the dielectronic recombination rates for certain ionization stages because of the neglect of the effects of an autoionization process, not previously discussed, in which the excited recombining ion core undergoes a $\Delta n = 0$ single-electron electric-dipole transition to a lower excited state. The new dielectronic recombination rates are used to calculate the corona ionization equilibrium distributions. Finally, these distributions are employed, in conjunction with reliable distorted wave results for the electron impact excitation rates (Davis et al. 1977), in a new evaluation of the radiative energy loss rates.

II. Theory of Dielectronic Recombination

Dielectronic recombination of the ion X^{+Z} with residual charge Z is the result of a radiationless capture into a doubly-excited state j, $n\ell$ of $X^{+(Z-1)}$

$$X^{+Z}(i) + e^{-}(\varepsilon_i \ell_i) \rightarrow X^{+(Z-1)}\ (j,n\ell) \qquad (1)$$

followed by a stabilizing radiative transition to a state k, nℓ which lies below the ionization threshold

$$X^{+(Z-1)}\ (j,\ n\ell) \rightarrow X^{+(Z-1)}\ (k,\ n\ell) + \hbar\,\omega. \tag{2}$$

In the corona model, the recombining ions are assumed to be initially in their ground states (i = g). In addition, the most important stabilizing radiative transitions will return the recombining ion core to its ground state configuration (k = g). In this investigation the many-electron states i, j, and k will be specified by the effective principal and angular momentum quantum numbers of the active electron.

For a Maxwellian electron velocity distribution the dielectronic recombination rate coefficient into the final state k, nℓ can be expressed in the form (Shore 1969)

$$\alpha_d\ (Z,\ i \rightarrow Z\text{-}1;\ k,\ n\ell) = 2^3\ a_o^3\ \pi^{3/2}\ \ (E_H/k_B\ T_e)^{3/2}$$

$$\times \sum_j \frac{g(Z\text{-}1;\ j,n\ell)}{2\ g(Z,i)}\ \ \frac{A_a(j,n\ell \rightarrow i,\varepsilon_i)\ \ A_r(j,n\ell \rightarrow k,n\ell)}{A(Z\text{-}1;\ j,n\ell)} \tag{3}$$

$$\times \exp\left[\frac{E(Z,i)\ -\ E(Z\text{-}1;\ j,n\ell)}{k_B\ T_e}\right].$$

The statistical weights associated with the energy levels E (Z,i) and E (Z-1; j,nℓ) are denoted by g (Z,i) and g (Z-1; j,nℓ) and $E_H = 13.6$ ev.

For $Z \leq 20$ dielectronic recombination occurs primarily through transitions involving highly excited nℓ states of the outer electron, especially when the recombining ion core undergoes a $\Delta n = o$ transition. Consequently, the autoionization rate $A_a(j,n\ell \rightarrow i, \varepsilon_i)$, in terms of which

the radiationless capture rate has been expressed, can be obtained from the threshold values of the partial wave electron impact excitation cross sections $\sigma\ (i,\varepsilon_i\ \ell_i \rightarrow j,\ \varepsilon_j\ \ell_j)$ by means of the quantum defect theory relationship (Seaton 1969)

$$A_a(j,\ n\ell \rightarrow\ i,\varepsilon_i) = \frac{E_H}{\hbar}\ \frac{2Z^2}{\pi^2\ n^3\ a_o^2}$$

$$X \left[\frac{E(Z,j)\ -\ E(Z,i)}{E_H}\right]\ \frac{1}{2(2\ell+1)}\ \frac{g(Z,i)}{g(Z,j)} \qquad (4)$$

$$X \sum_{\ell_i}\ \sigma(i,\varepsilon_i\ \ell_i \rightarrow j,\ \varepsilon_j\ \ell)\Big|_{\varepsilon_j\,=\,o}\ .$$

In addition, the spontaneous radiative transition rate $A_r(j,\ n\ell \rightarrow k,\ n\ell)$ can be calculated by neglecting the influence of the outer $n\ell$ electron.

The essential innovation in the present investigation is the correct determination of the total decay rate $A(Z\text{-}1;\ j,\ n\ell)$. A careful examination of the general theory has revealed (JDKB) that the total decay rate of the doubly-excited state $j,\ n\ell$ must be determined by taking into consideration the autoionization rates $A_a(j,\ n\ell \rightarrow k,\varepsilon_k)$ into all lower states k of the recombining ion and the spontaneous radiative transition rates $A_r(j,\ n\ell \rightarrow k,\ n\ell)$ and $A_r(j,\ n\ell \rightarrow k,\varepsilon_k)$ into all lower bound states $k,\ n\ell$ and continuum states $k,\ \varepsilon_k$.

$$A(Z\text{-}1;\ j,\ n\ell) = \sum_{k<j} \left[A_a(j,\ n\ell \rightarrow k,\ \varepsilon_k) + A_r(j,\ n\ell \rightarrow k,\ n\ell) + \int d\varepsilon_k\ A_r(j,\ n\ell \rightarrow k,\ \varepsilon_k) \right] . \quad (5)$$

In previous calculations it has been assumed that the doubly-excited states which give the most important contributions to the total dielectronic recombination rate undergo autoionization with the greatest probability into the ground state of the recombining ion. While the most probable radiative decay process usually terminates in the ground state, the corresponding assumption for autoionization is invalid for the most important doubly-excited states of certain ions. In the boron-like through the neon-like ions, for example, the 3d, $n\ell$ doubly-excited states are found to autoionize preferentially into the lower excited 3p state rather than into the 2p ground state, from which radiationless capture is assumed to occur. This is illustrated in Figure 1 by using long and short arrows to indicate the alternative autoionization channels. Because capture from the 3p excited state is negligible at low densities, as indicated by the absence of the corresponding arrow in Figure 1, the inclusion of the additional 3d → 3p autoionization rate must lead to a reduction of the 3d → 2p contribution to the dielectronic recombination rate.

Previous investigations of dielectronic recombination contain no discussion of the role of radiative Auger transitions (Åberg 1971) in the determination of the total decay widths $A(Z\text{-}1;\ j,\ n\ell)$. Using quantum defect theory (Seaton 1969) the total contribution from radiative Auger transitions of the type

$$X^{+(Z-1)}\ (j,\ n\ell) \rightarrow X^{+(Z)}\ (k) + e^{-}\ (\varepsilon_k \ell_k) + \hbar\omega \qquad (6)$$

is found to satisfy the inequality

$$\int d\varepsilon_k\ A_r(j,\ n\ell \rightarrow k,\ \varepsilon_k) < \frac{2Z^2}{\pi^2 n^3}\ A_r(j \rightarrow k). \qquad (7)$$

It follows that for large n-values the radiative Auger contribution to the total decay width can be neglected provided Z is not too large.

The basic approximation in the theory of dielectronic recombination is that the total spontaneous radiative capture rate coefficient $\alpha\ (Z,\ i \rightarrow Z\text{-}1;\ k,\ n\ell)$ into the final state k, $n\ell$ can be obtained simply by adding to the dielectronic contribution given by equation (3) the direct radiative recombination rate coefficient describing the free-bound transition of a single-electron. A formula for estimating the direct radiative recombination rate, which takes into account the presence of equivalent electrons in the outer subshell of the recombining ion, has been given previously (JDKB). The interference between the direct radiative and dielectronic recombination amplitudes, which occurs in the exact expression for the quantum mechanical transition amplitude, can be neglected because each separate contribution is almost always dominant in a temperature region in which the other contribution is negligible.

III. The Overall Recombination Coefficients For Low-Density Plasmas

In the zero-density limit the overall recombination rate coefficient simply equals the total rate coefficient for all spontaneous radiative captures, by both single-and by two- electron transitions

$$\alpha(Z,\ i \rightarrow Z\text{-}1) = \sum_{k,n\ell} \alpha(Z,\ i \rightarrow Z\text{-}1;\ k,\ n\ell). \qquad (8)$$

At any given finite density there will be some limiting n-value above which subsequent collisional excitation of the final state k, $n\ell$ becomes as probable as radiative decay to lower levels. It can be argued that levels above this limit should not be included in equation (8), but termination of the summation over n at the limiting value obtained from the formula given by Griem (1964) probably results in an overestimate of the finite density reduction of the recombination rate. In the present investigation the limiting n-value has been determined by the less restrictive condition (Inglis and Teller 1939) that the quasi-static linear-Stark shifts produced by all surrounding charged-particles must not exceed the separation between levels with adjacent n-values.

When the cut-off procedure affects the outer electron $n\ell$- levels which play the most important role in the dielectronic recombination process, a more fundamental treatment of the density-dependence is required. Burgess and Summers (1969) solved a set of statistical equilibrium equations which describes the effects of collisions on the final state populations and calculated a density-dependent overall recombination coefficient by a procedure similar to that employed by Bates et al. (1962). However, this treatment of density-dependent dielectronic recombination is incomplete because no account is taken of the influence of the plasma on the doubly-excited level populations (Jacobs, Davis and Kepple 1976).

The dielectronic recombination rate coefficients for the various ions of silicon have been calculated with account taken of all stabilizing radiative transitions and all autoionization processes which involve a single-electron electric-dipole transition of the recombining ion core. A distorted wave calculation (Davis et al. 1977) was employed to obtain the threshold values of the collisional excitation cross sections, because the widely-used Bethe approximation is known to greatly overestimate the most important partial wave contributions. In Table I the stabilizing radiative transitions $j \rightarrow k$ are given in order of decreasing importance at the temperature where the ion in question is predicted by the present calculations to have its maximum equilibrium abundance. The asterisk has been used to identify the transitions which involve doubly-excited states subject to autoionization into an excited state of the recombining ion.

In Table II the dielectronic contributions to the overall recombination rate coefficients are presented as functions of $\log_{10} T_e(^{\circ}K)$. Also given are the values which were obtained by evaluating the Burgess formula with our nonhydrogenic energy eigenvalues and oscillator strengths for the transitions in Table I. The effects of the surrounding charged particles in a plasma with an electron density of 10^{10} cm^{-3} have been estimated by terminating the summation over n in equation (8) at the Inglis-Teller limit. The limiting n-value obtained from the Inglis-Teller criterion increases with Z as $Z^{3/5}$, whereas for a given stabilizing radiative transtion $j \rightarrow k$ the n-values which give the dominant contribution to the total dielectronic recombination rate are descreasing with increasing Z. Consequently, the recombination rates obtained for the most

highly-charged ions are to a good approximation independent of density over an extensive density range. Three-body recombination is negligible at the densities of interest.

In the temperature regions of maximum equilibrium abundance, the dielectronic recombination rate coefficients obtained from the present calculation are in several cases substantially reduced in comparison with the values obtained from the Burgess formula. For Si V - Si X this reduction is attributable to the effect of autoionization into the 3p excited state of the recombining ion, which is found to be the dominant autoionization process for the 3d, $n\ell$ doubly-excited states.

The effect of autoionization accompanied by excitation is illustrated in Figure 2 by showing as functions of $\log_{10} T_e(^{\circ}K)$ the contributions to the Si VI overall recombination coefficient arising from the direct radiative transition and from the three most important dielectronic transitions. When no account is taken of autoionization into the 3p excited state, the dielectronic contribution arising from the 3d → 2p radiative transition is found to be dominant in the maximum equilibrium abundance temperature region. This is illustrated by the values obtained using the Burgess formula, which are in this case about two orders of magnitude larger than the present results. With the inclusion of the additional 3d → 3p autoionization rate, the 3s → 2p and 2p → 2s dielectronic contributions are relatively more important.

IV. Corona Ionization Equilibrium

The corona equilibrium distributions of the ions of a given element are determined by the conditions

$$N(Z-1,g)\ S(Z-1,g \rightarrow Z) = N(Z,g)\ \alpha(Z,g \rightarrow Z-1),\ 1 \leq Z \leq Z_{max} \qquad (9)$$

together with the normalization requirement

$$N_T = \sum_{Z=0}^{Z_{max}} N(Z,g) \qquad (10)$$

$N(Z,g)$ is the density of ions with residual charge Z in the ground state, while N_T is the total density. $S(Z-1,\ g \rightarrow Z)$ denotes the total rate coefficient for single ionization from the ground state of $X^{(Z-1)}$ as a result of thermal electron impacts. $\alpha(Z,\ g \rightarrow Z-1)$ is the overall recombination rate coefficient from the ground state of $X^{(Z)}$. When three-body recombination and the density dependence of the spontaneous radiative capture rate discussed in the preceding section are neglected, the relative abundances $N\ (Z,g)/N_T$ are independent of density and are functions only of the local electron temperature.

The ionization rate coefficients employed in the present calculations were obtained by evaluating the semi-empirical expression given by Lotz (1967). Contributions from inner-shell ionization have been included. The additional contributions from autoionization following inner-shell excitation have been estimated by using a procedure similar to the one employed by Jordan (1969). Experimentally determined (Datla, Nugent, and Griem 1976) ionization rate coefficients for certain multiply-charged ions are as much as a factor of 2 less than the predictions of the semi-empirical formula. This uncertainty is, however, small compared to the reductions which have been obtained in the overall recombination rates by the inclusion of autoionization accompanied by excitation.

The relative steady-state abundances of the various ions of silicon are presented in Table III and shown in Figure 3 as functions of $\log_{10} T_e$ (^{o}K). The maximum equilibrium abundance temperatures are given in Table IV together with those predicted by the calculations of Jordan (1969) and Summers (1974). The differences between the results of the two previous calculations are most probably attributable to the use of different ionization rate coefficients. Very close agreement with the results of Jordan (1969) is obtained in the present calculations by the omission of the rates for autoionization into an excited state. Consequently the shifts in the abundance curves toward lower temperatures, which are illustrated for Si V - Si VII in Figure 4, are directly attributable to the effects of autoionization accompanied by excitation. The reduced maximum abundance temperatures which have been obtained for certain ions are still significantly higher than those predicted (House 1964) when no account is taken of the effects of dielectronic recombination. It should be emphasized that a relatively small shift of a sharply peaked abundance curve can significantly alter the predicted emission line intensity.

V. Radiative Energy Loss Rates

In this section the results are presented for the rates of radiative energy loss arising from radiation processes which involve collisions between silicon ions and thermal electrons. The ions are assumed to be in corona ionization equilibrium, and no account is taken of the effects of self-absorption.

The rate at which energy is radiated per unit volume as a result of the electron impact excitation of the resonance lines is given by

$$\epsilon_L = N_e N_T \sum_{Z=1}^{Z_{max}-1} \frac{N(Z,g)}{N_T} \sum_j \Delta E(Z,g \rightarrow j)\, C(Z,g \rightarrow j)\, B(Z,j \rightarrow g) \qquad (11)$$

The excitation energies are denoted by $\Delta E(Z,g \rightarrow j)$, and $C(Z,g \rightarrow j)$ are the collisional excitation rate coefficients obtained from the distorted wave calculation (Davis et al. 1977). The branching ratios $B(Z,j \rightarrow g)$ for the resonance line emissions are very close to unity.

The total power radiated per unit volume during dielectronic recombination is given by

$$\epsilon_d = N_e N_T \sum_{Z=1}^{Z_{max}-1} \frac{N(Z,g)}{N_T} \sum_j \Delta E(Z,g \rightarrow j)\, \alpha_d(Z,g;\, j \rightarrow g), \qquad (12)$$

where α_d $(Z, g; j \rightarrow g)$ denotes the contribution to the overall dielectronic recombination rate coefficient arising from the stabilizing radiative transition $j \rightarrow g$. No account has been taken of the radiation which is emitted when the $n\ell$-states of the outer electron cascade to the ground states. In addition, we have neglected the displacement of the emitted photon frequency from the center of the resonance line which results from the presence of the outer electron. The single-electron electric-dipole transitions in Table I have been taken into account in the evaluation of both the resonance line and the dielectronic recombination contributions.

The results are presented in Figure 5 by plotting as functions of $\log_{10} T_e$ (^oK) the rate coefficients $\epsilon_L/N_e N_T$ and $\epsilon_d/N_e N_T$, which have the dimensions of power X volume. Also shown are the corresponding rate

coefficients for direct recombination radiation and for bremsstrahlung which were evaluated as described by Griem (1964). The relative maximum produced by the 2p → 2s transitions in Si VI - Si XII is found to occur very close to 10^6 °K, which is lower than predicted by the calculations of Cox and Tucker (1969). This reduction is directly attributable to the effects of the reduced recombination rates on the ionization equilibrium distributions.

In Table V the individual contributions to the rate coefficients $\epsilon_L/N_e N_T$ and $\epsilon_d/N_e N_T$ from the most important radiative transitions j → g are given at the maximum line emission temperatures, which are in several cases significantly higher than the maximum abundance temperatures in Table IV. The intensity of dielectronic recombination radiation, relative to the associated resonance line intensity, is found to be greatest in the cases of the 2p → 1s transitions of the helium-like and hydrogen-like ions Si XIII and Si XIV. It has been pointed out by Gabriel (1972) that for higher members of the helium isoelectronic sequence the dielectronic recombination process occurs primarily through the n = 2 levels of the outer electron, which give rise to satellite features that are spectroscopically resolvable from the resonance line.

Although the radiation emitted during dielectronic recombination can be considerably more important than direct recombination radiation and bremsstrahlung, the electron impact excitation of resonance line radiation is clearly the dominant radiative cooling mechanism at temperatures where ions with bound electrons are abundant. In a rapidly ionizing plasma the ionization of multiply-charged ions may represent an important energy loss mechanism. Resonance line emission is expected to be the dominant energy loss mechanism for multiply-charged ions in ionization equilibrium.

VI. Conclusions

With account taken of the effects of autoionization accompanied by excitation, the present calculation for the dielectronic recombination rates and the ionization equilibrium distributions may represent the best improvement that is possible within the single-electron electric-dipole and simple corona model approximations. The use of a more sophisticated calculation for the ionization rates would be desirable. However, the most significant additional improvements are expected to result from taking into account more general autoionization and radiation processess in a treatment of the effects of collisions on both the singly- and the doubly- excited level populations. This more sophisticated treatment of dielectronic recombination will be the subject of a future investigation.

ACKNOWLEDGMENTS

This work has been supported by the E. O. Hulbert Center for Space Research, NRL, as part of the ATM Data Analysis Program funded by NASA

Table I

Stabilizing Radiative Transitions in Order of Decreasing Importance at the Temperature of Maximum Equilibrium Abundance

Recombining Ion	Single - Electron Transitions			
Si II	$3p \rightarrow 3s$,	$4d \rightarrow 3p^*$,	$4s \rightarrow 3p$,	$3d \rightarrow 3p$
Si III	$3p \rightarrow 3s$,	$4p \rightarrow 3s^*$		
Si IV	$3p \rightarrow 3s$,	$4p \rightarrow 3s^*$		
Si V	$3s \rightarrow 2p$,	$3d \rightarrow 2p^*$		
Si VI	$3s \rightarrow 2p$,	$2p \rightarrow 2s$,	$3d \rightarrow 2p^*$	
Si VII	$2p \rightarrow 2s$,	$3d \rightarrow 2p^*$,	$3s \rightarrow 2p$	
Si VIII	$2p \rightarrow 2s$,	$3d \rightarrow 2p^*$,	$3s \rightarrow 2p$	
Si IX	$2p \rightarrow 2s$,	$3d \rightarrow 2p^*$,	$3s \rightarrow 2p$	
Si X	$2p \rightarrow 2s$,	$3d \rightarrow 2p^*$,	$3s \rightarrow 2p$	
Si XI	$2p \rightarrow 2s$,	$3p \rightarrow 2s^*$		
Si XII	$2p \rightarrow 2s$,	$3p \rightarrow 2s^*$		
Si XIII	$2p \rightarrow 1s^*$			

*Affected by Autoionization Accompanied by Excitation

Table II

Dielectronic Recombination Rate Coefficients (cm^3 sec^{-1})

$\log_{10} T_e$ (°K)	Recombining Ions					
	Si II	Si III	Si IV	Si V	Si VI	Si VII
4.0	0.16(-11)*	0.49(-12)	0.54(-11)	0.63(-37)	0.15(-17)	0.18(-19)
	0.44(-10)**	0.66(-11)	0.56(-12)	0.46(-38)	0.42(-33)	0.33(-31)
4.2	0.54(-11)	0.48(-11)	0.11(-10)	0.70(-28)	0.17(-15)	0.44(-16)
	0.77(-10)	0.46(-10)	0.12(-10)	0.61(-27)	0.17(-24)	0.10(-22)
4.4	0.13(-10)	0.27(-10)	0.34(-10)	0.36(-22)	0.26(-14)	0.47(-14)
	0.99(-10)	0.14(-9)	0.69(-10)	0.49(-20)	0.36(-19)	0.18(-17)
4.6	0.20(-10)	0.70(-10)	0.66(-10)	0.25(-18)	0.12(-13)	0.76(-13)
	0.10(-9)	0.26(-9)	0.16(-9)	0.86(-16)	0.65(-16)	0.29(-14)
4.8	0.20(-10)	0.10(-9)	0.81(-10)	0.93(-16)	0.30(-13)	0.56(-12)
	0.84(-10)	0.32(-9)	0.22(-9)	0.32(-13)	0.60(-14)	0.23(-12)
5.0	0.16(-10)	0.99(-10)	0.72(-10)	0.52(-14)	0.10(-12)	0.34(-11)
	0.59(-10)	0.28(-9)	0.21(-9)	0.10(-11)	0.14(-12)	0.29(-11)
5.2	0.11(-10)	0.76(-10)	0.52(-10)	0.94(-13)	0.34(-12)	0.11(-10)
	0.37(-10)	0.20(-9)	0.16(-9)	0.74(-11)	0.19(-11)	0.11(-10)
5.4	0.65(-11)	0.50(-10)	0.33(-10)	0.59(-12)	0.84(-12)	0.20(-10)
	0.22(-10)	0.13(-9)	0.11(-9)	0.22(-10)	0.10(-10)	0.23(-10)
5.6	0.36(-11)	0.30(-10)	0.19(-10)	0.16(-11)	0.17(-11)	0.23(-10)
	0.12(-10)	0.76(-10)	0.63(-10)	0.39(-10)	0.28(-10)	0.40(-10)
5.8	0.20(-11)	0.17(-10)	0.10(-10)	0.23(-11)	0.27(-11)	0.21(-10)
	0.64(-11)	0.42(-10)	0.35(-10)	0.47(-10)	0.45(-10)	0.60(-10)
6.0	0.10(-11)	0.89(-11)	0.55(-11)	0.23(-11)	0.29(-11)	0.17(-10)
	0.33(-11)	0.22(-10)	0.19(-10)	0.44(-10)	0.49(-10)	0.68(-10)
6.2	0.53(-12)	0.47(-11)	0.29(-11)	0.18(-11)	0.24(-11)	0.12(-10)
	0.17(-11)	0.12(-10)	0.98(-11)	0.33(-10)	0.41(-10)	0.59(-10)
6.4	0.27(-12)	0.24(-11)	0.15(-11)	0.12(-11)	0.17(-11)	0.76(-11)
	0.87(-12)	0.60(-11)	0.50(-11)	0.22(-10)	0.28(-10)	0.43(-10)
6.6	0.14(-12)	0.12(-11)	0.75(-12)	0.71(-12)	0.10(-11)	0.45(-11)
	0.44(-12)	0.30(-11)	0.26(-11)	0.13(-10)	0.18(-10)	0.27(-10)

Table II (continued)

$\log_{10} T_e$ (°K)	Recombining Ions					
	Si VIII	Si IX	Si X	Si XI	Si XII	Si XIII
5.0	0.13(-10)	0.27(-10)	0.37(-10)	0.43(-10)	0.36(-10)	
	0.12(-10)	0.23(-10)	0.34(-10)	0.33(-10)	0.47(-10)	
5.2	0.27(-10)	0.46(-10)	0.65(-10)	0.78(-10)	0.44(-10)	
	0.28(-10)	0.47(-10)	0.68(-10)	0.78(-10)	0.57(-10)	
5.4	0.36(-10)	0.55(-10)	0.77(-10)	0.10(-9)	0.40(-10)	
	0.38(-10)	0.58(-10)	0.82(-10)	0.10(-9)	0.51(-10)	
5.6	0.34(-10)	0.49(-10)	0.68(-10)	0.94(-10)	0.29(-10)	0.79(-28)
	0.43(-10)	0.54(-10)	0.72(-10)	0.98(-10)	0.37(-10)	0.45(-29)
5.8	0.28(-10)	0.38(-10)	0.50(-10)	0.71(-10)	0.19(-10)	0.11(-21)
	0.53(-10)	0.53(-10)	0.58(-10)	0.77(-10)	0.25(-10)	0.82(-22)
6.0	0.21(-10)	0.27(-10)	0.34(-10)	0.46(-10)	0.11(-10)	0.71(-18)
	0.63(-10)	0.57(-10)	0.48(-10)	0.60(-10)	0.21(-10)	0.24(-17)
6.2	0.15(-10)	0.19(-10)	0.22(-10)	0.28(-10)	0.69(-10)	0.21(-15)
	0.59(-10)	0.52(-10)	0.40(-10)	0.49(-10)	0.20(-10)	0.13(-14)
6.4	0.10(-10)	0.13(-10)	0.14(-10)	0.16(-10)	0.42(-11)	0.85(-14)
	0.46(-10)	0.42(-10)	0.31(-10)	0.37(-10)	0.18(-10)	0.52(-13)
6.6	0.61(-11)	0.78(-11)	0.84(-11)	0.86(-11)	0.24(-11)	0.82(-13)
	0.30(-10)	0.28(-10)	0.21(-10)	0.25(-10)	0.13(-10)	0.43(-12)
6.8	0.35(-11)	0.45(-11)	0.48(-11)	0.46(-11)	0.14(-11)	0.28(-12)
	0.18(-10)	0.17(-10)	0.13(-10)	0.16(-10)	0.87(-11)	0.12(-11)
7.0	0.19(-11)	0.25(-11)	0.26(-11)	0.24(-11)	0.76(-12)	0.49(-12)
	0.10(-10)	0.98(-11)	0.72(-11)	0.92(-11)	0.52(-11)	0.19(-11)
7.2	0.10(-11)	0.13(-11)	0.14(-11)	0.12(-11)	0.40(-12)	0.52(-12)
	0.55(-11)	0.53(-11)	0.39(-11)	0.50(-11)	0.29(-11)	0.19(-11)
7.4	0.52(-12)	0.69(-12)	0.71(-12)	0.63(-12)	0.21(-12)	0.44(-12)
	0.29(-11)	0.28(-11)	0.21(-11)	0.27(-11)	0.16(-11)	0.15(-11)
7.6	0.27(-12)	0.35(-12)	0.37(-12)	0.32(-12)	0.11(-12)	0.30(-12)
	0.15(-11)	0.14(-11)	0.11(-11)	0.14(-11)	0.82(-12)	0.99(-12)

* Numbers in parentheses are the powers of 10.

** Calculated using the formula of Burgess (1965).

Table III

$-\log_{10} N(Z)/N_T$ for Silicon Ions

$\log_{10} T_e$ (°K)	Si II	Si III	Si IV	Si V	
4.0	0.06	4.34			
4.1	0.02	2.76			
4.2	0.01	1.73			
4.3	0.04	1.04			
4.4	0.13	0.58	5.00		
4.5	0.30	0.29	3.43		
4.6	0.56	0.14	2.25	4.94	
4.7	0.87	0.09	1.34	2.74	
4.8	1.28	0.17	0.72	1.05	
4.9	2.20	0.77	0.73	0.19	
5.0	3.54	1.84	1.27	0.03	
5.1	4.82	2.86	1.85	0.01	
5.2		3.73	2.33	0.01	

$\log_{10} T_e$ (°K)	Si V	Si VI	Si VII	Si VIII	Si IX
5.0	0.03				
5.1	0.01	3.63			
5.2	0.01	2.17			
5.3	0.04	1.06	4.30		
5.4	0.23	0.37	2.58		
5.5	0.66	0.12	1.49	3.93	
5.6	1.17	0.11	0.77	2.34	5.00
5.7	1.76	0.30	0.37	1.21	2.98
5.8	2.53	0.72	0.30	0.54	1.57
5.9	3.50	1.41	0.57	0.31	0.73
6.0	4.70	2.34	1.14	0.45	0.37
6.1		3.51	1.99	0.95	0.45
6.2		5.00	3.24	1.88	1.02

Table III (continued)

$\log_{10} T_e$ (°K)	Si X	Si XI	Si XII	Si XIII	Si XIV	Si XV
6.0	0.86	1.90	3.10	4.43		
6.1	0.44	0.92	1.50	2.16		
6.2	0.60	0.60	0.65	0.76		
6.3	1.38	0.97	0.58	0.23		
6.4	2.36	1.60	0.82	0.08	4.27	
6.5	3.28	2.20	1.10	0.04	3.14	
6.6	4.12	2.74	1.36	0.02	2.26	
6.7	4.85	3.22	1.58	0.03	1.58	3.89
6.8		3.65	1.78	0.04	1.07	2.71
6.9		4.07	1.98	0.10	0.71	1.80
7.0		4.50	2.21	0.22	0.48	1.11
7.1		5.00	2.53	0.43	0.39	0.63
7.2			2.93	0.74	0.44	0.34

Table IV

Maximum Equilibrium Abundance Temperatures (in ^{o}K) for Silicon Ions

Ion	Present Results	Jordan (1969)	Summers (1974)
Si II	1.6(4)	1.6(4)	1.6(4)
Si III	5.0(4)	5.0(4)	6.3(4)
Si IV	6.3(4)	8.0(4)	8.0(4)
Si V	1.6(5)	2.0(5)	2.0(5)
Si VI	4.0(5)	5.0(5)	5.0(5)
Si VII	6.3(5)	7.0(5)	1.0(6)
Si VIII	8.0(5)	1.0(6)	1.3(6)
Si IX	1.0(6)	1.3(6)	1.6(6)
Si X	1.3(6)	1.6(6)	2.0(6)
Si XI	1.6(6)	2.0(6)	2.5(6)
Si XII	2.0(6)	2.0(6)	2.5(6)
Si XIII	4.0(6)	4.0(6)	4.0(6)
Si XIV	1.3(6)	1.3(7)	1.3(7)

* Numbers in parentheses are the powers of 10.

Table V

Individual Contributions to the Energy Loss Coefficients for Dielectronic Recombination and Line Radiation, evaluated at the Maximum Line Emission Temperature

Ion	Radiative Transition $j \rightarrow k$*	Maximum Line Emission Temperature (^{o}K)	$\epsilon_d/N_e N_T$ (Watts cm^3)	$\epsilon_L/N_e N_T$ (Watts cm^3)
Si II	3p → 3s	2.5(4)**	0.90(-29)	0.24(-25)
	4d → 3p	2.5(4)	0.58(-30)	0.12(-25)
Si III	3p → 3s	6.3(4)	0.11(-27)	0.12(-24)
	4p → 3s	6.3(4)	0.80(-30)	0.12(-24)
Si IV	3p → 3s	8.0(4)	0.32(-28)	0.22(-25)
	4p → 3s	8.0(4)	0.20(-30)	0.96(-26)
Si V	3s → 2p	2.5(5)	0.49(-29)	0.16(-27)
	3d → 2p	3.2(5)	0.34(-30)	0.57(-27)
Si VI	2p → 2s	4.0(5)	0.36(-29)	0.33(-27)
	3s → 2p	5.0(5)	0.11(-28)	0.50(-27)
	3d → 2p	5.0(5)	0.49(-29)	0.36(-26)

Table V (continued)

Si VII	2p → 2s 3s → 2p 3d → 2p	6.3(5) 6.3(5) 6.3(5)	0.75(-28) 0.13(-28) 0.23(-28)	0.90(-26) 0.46(-27) 0.55(-26)
Si VIII	2p → 2s 3s → 2p 3d → 2p	8.0(5) 1.0(6) 1.0(6)	0.60(-28) 0.12(-28) 0.42(-28)	0.13(-25) 0.45(-27) 0.63(-26)
Si IX	2p → 2s 3s → 2p 3d → 2p	1.0(6) 1.3(6) 1.3(6)	0.54(-28) 0.97(-29) 0.64(-28)	0.13(-25) 0.32(-27) 0.57(-26)
Si X	2p → 2s 3s → 2p 3d → 2p	1.3(6) 1.6(6) 1.6(6)	0.47(-28) 0.40(-29) 0.42(-28)	0.14(-25) 0.11(-27) 0.27(-26)
Si XI	2p → 2s 3p → 2s	1.6(6) 1.6(6)	0.45(-28) 0.85(-29)	0.12(-25) 0.20(-26)
Si XII	2p → 2s 3p → 2s	2.0(6) 2.0(6)	0.35(-29) 0.13(-28)	0.38(-26) 0.14(-26)
Si XIII	2p → 1s	1.0(6)	0.66(-28)	0.22(-26)
Si XIV	2p → 1s	1.6(6)	0.16(-27)	0.13(-26)

* Including all LS- Components.

** Numbers in parentheses are the powers of 10.

References

Aberg, T. 1971, Phys. Rev. A, 4, 1735.

Bates, D. R., Kingston, A. E., and R. W. P. Mc Whirter, Proc. Roy. Soc. (London) A, 267, 297 (1962).

Burgess, A. 1964, Ap. J., 139, 776.

Burgess, A. 1965, Ap. J., 141, 1588.

Burgess, A. and Summers, H. P. 1969, Ap. J., 157, 1007.

Cox, D. P. and Tucker, W. H. 1969, Ap. J., 157, 1157.

Datla, R. U., Nugent, L. J., and Griem, H. R. 1976, Phys. Rev. A, 14, 979.

Davis, J., Kepple, P. C., and M. Blaha, 1977, in preparation.

Gabriel, A. 1972, M. N. R. A. S., 160, 99.

Gabriel, A. H. and Jordan, C. 1972, Chapter 4 in Case Studies in Atomic Collision Physics II edited by E. W. Mc Daniel and M. R. C. Mc Dowell (North-Holland, New York).

Griem, H. R. 1964, Plasma Spectroscopy (New York: Mc Graw-Hill).

House, L. L. 1964, Ap. J. Suppl., 8, 307.

Inglis, D. R. and Teller, E. 1939, Ap. J., 90, 439.

Jacobs, V. L., Davis, J., Kepple, P. C., and Blaha, M., 1977, Ap. J., in press.

Jacobs, V. L., Davis, J., Kepple, P. C., 1976, submitted to Phys. Rev. Letters.

Jordan, C. 1969, M. N. R. A. S., 142, 501.

Lotz, W. 1967, Ap. J., Suppl., 14, 207.

McWhirter, R. W. P. 1965, in Plasma Diagnostic Techniques, edited by R. H. Huddlestone and S. L. Leonard (New York, Academic).

Seaton, M. J. 1964, J. Phys. B, 2, 5.

References Continued

Shore, B. W. 1969, Ap. J., 158, 1205.

Summers, H. P. 1974, M. N. R. A. S., 169, 1974.

Figure Captions

Figure 1. Radiationless capture, autoionization, and radiative decay processes determining the 3d, nℓ doubly-excited level populations in boron-like through neon-like ions.

Figure 2. Direct radiative and dielectronic contributions to the Si VI recombination rate coefficient.

_____ present calculation

- - - - - - - - - - - - Burgess formula (1965).

Figure 3. The corona ionization equilibrium of silicon ions.

Figure 4. The corona ionization equilibrium distributions for Si V - Si VII.

_____ present calculation

- - - - - - - - - - - - Jordan (1969).

Figure 5. The radiative energy loss rate coefficients for silicon ions in isothermal steady-state plasmas.

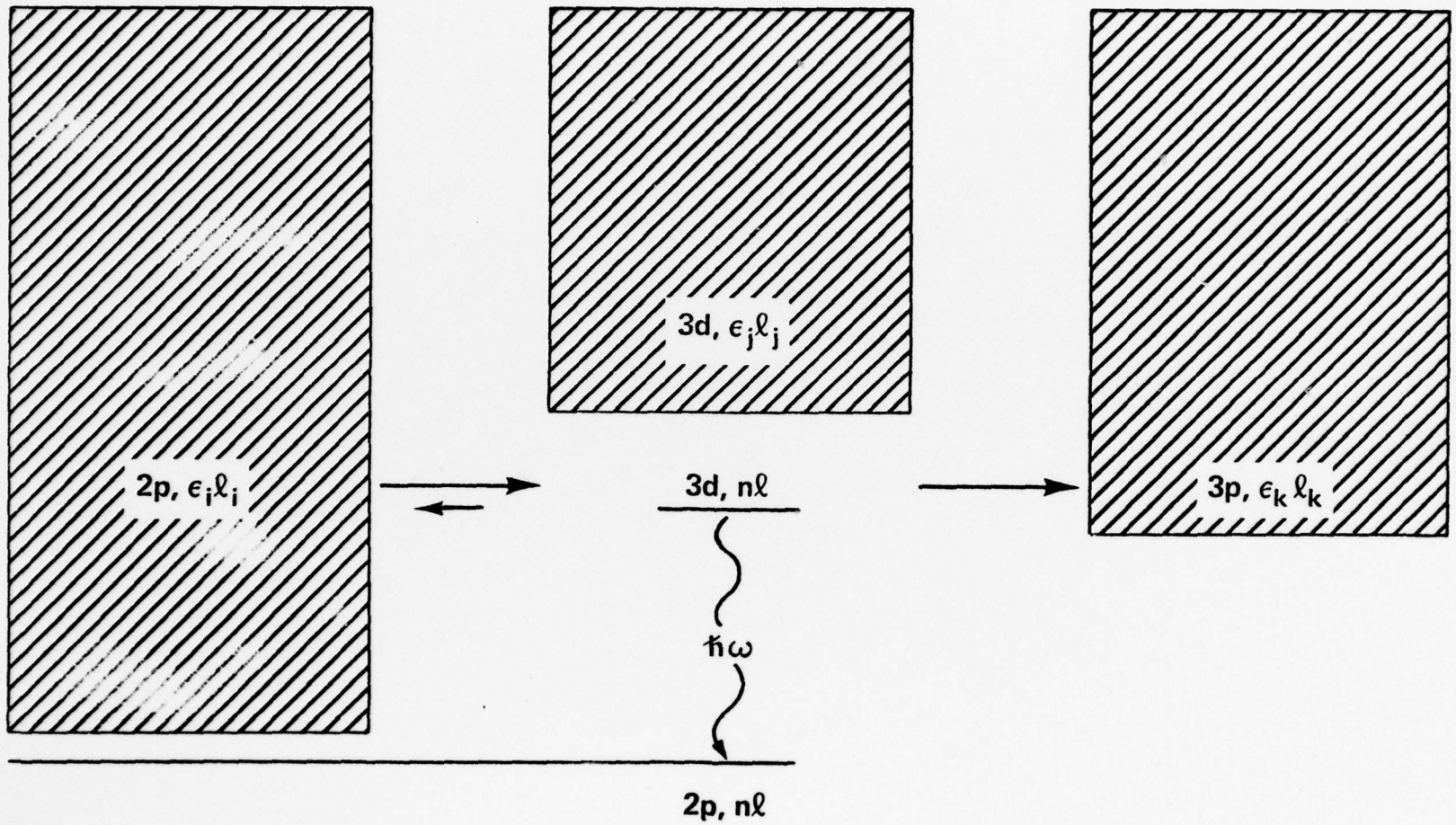
2p, $\epsilon_i \ell_i$
3d, $\epsilon_j \ell_j$
3d, $n\ell$
3p, $\epsilon_k \ell_k$
$\hbar\omega$
2p, $n\ell$

Fig. 1

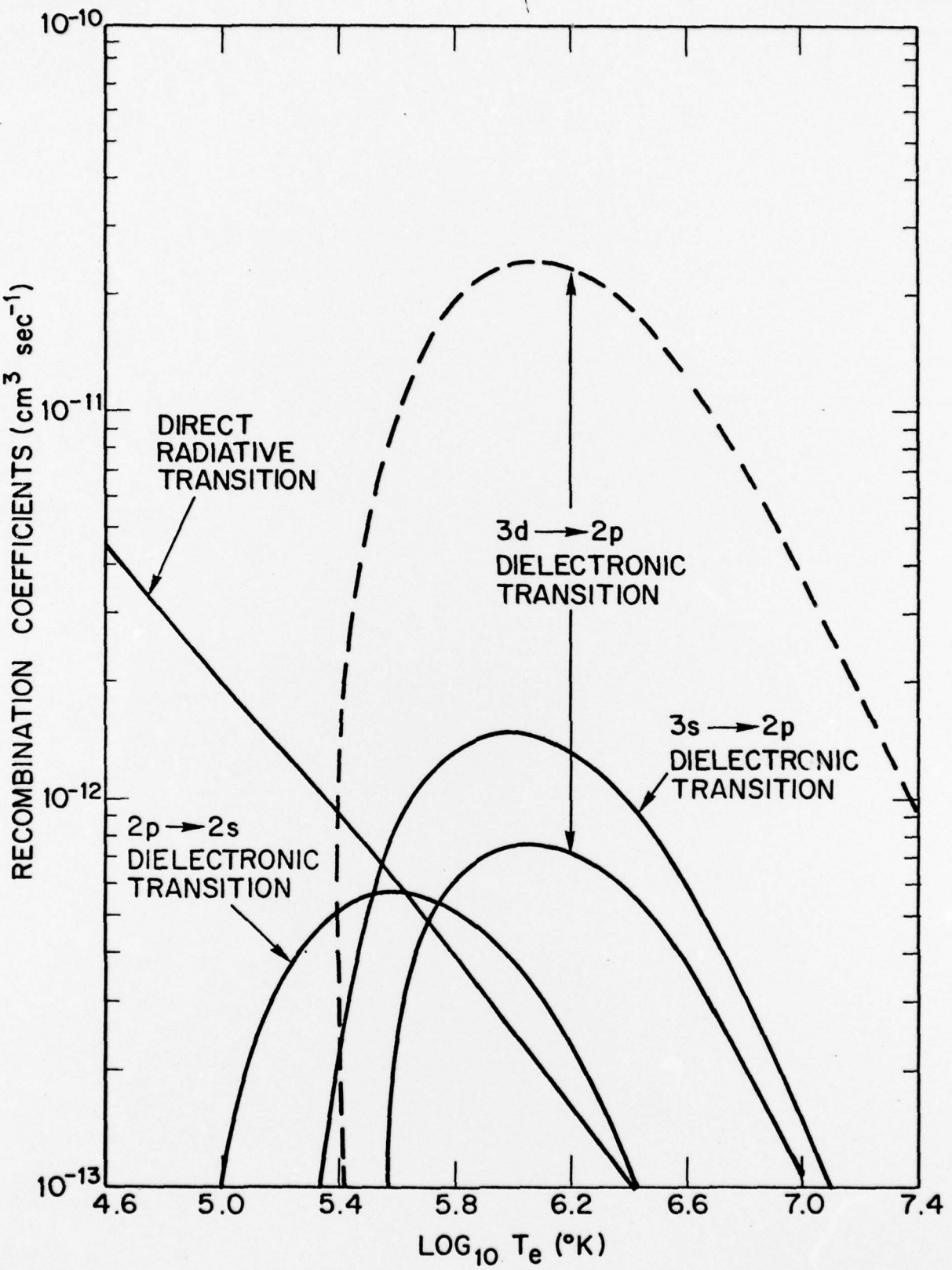
10^{-10}
10^{-11}
10^{-12}
10^{-13}
RECOMBINATION COEFFICIENTS (cm^3 sec^{-1})
DIRECT RADIATIVE TRANSITION
3d → 2p DIELECTRONIC TRANSITION
3s → 2p DIELECTRONIC TRANSITION
2p → 2s DIELECTRONIC TRANSITION
4.6
5.0
5.4
5.8
6.2
6.6
7.0
7.4
LOG_{10} T_e (°K)

Fig. 2

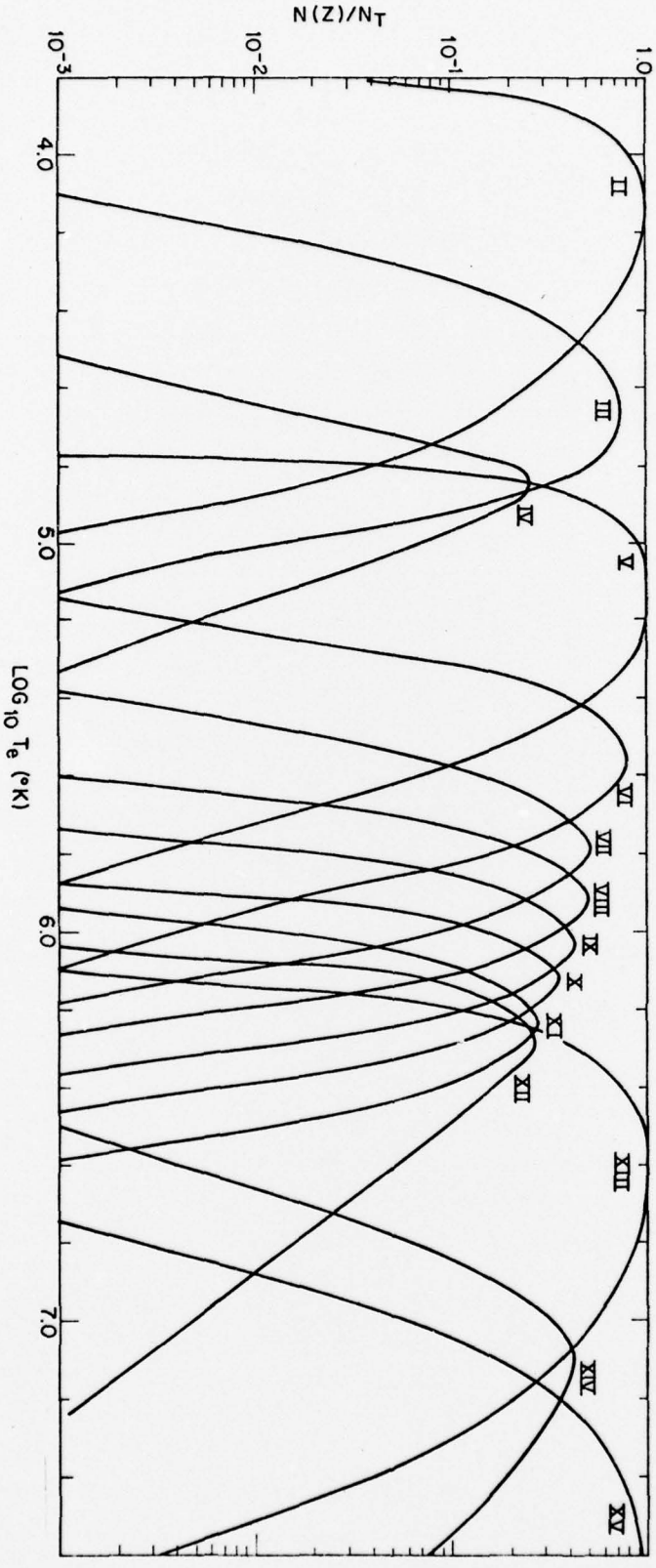
N(Z)/N_T
10^-3
10^-2
10^-1
1.0
4.0
5.0
6.0
7.0
LOG10 Te (°K)
II
III
IV
V
VI
VII
VIII
IX
X
XI
XII
XIII
XIV
XV

Fig. 3

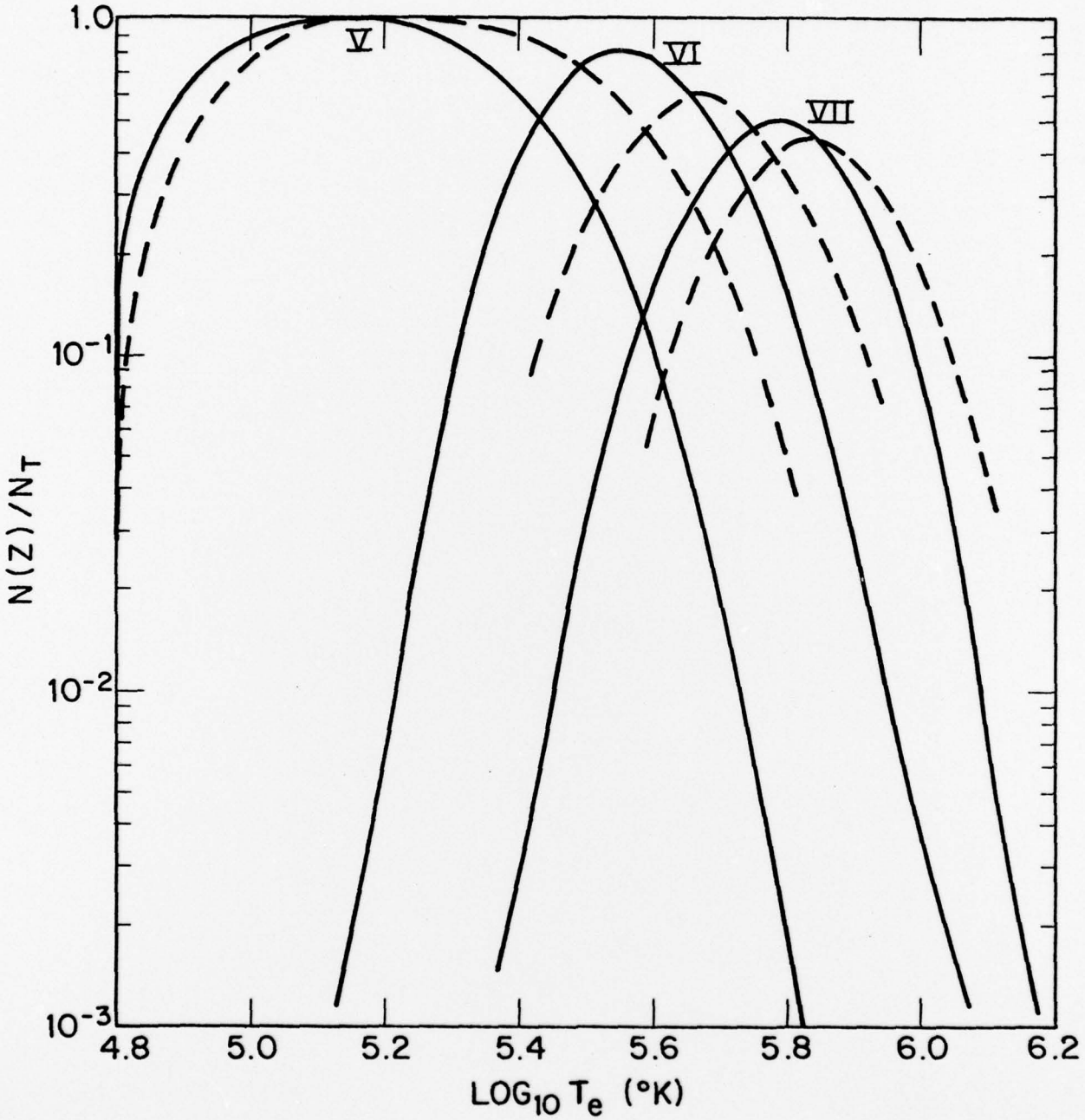

Fig. 4

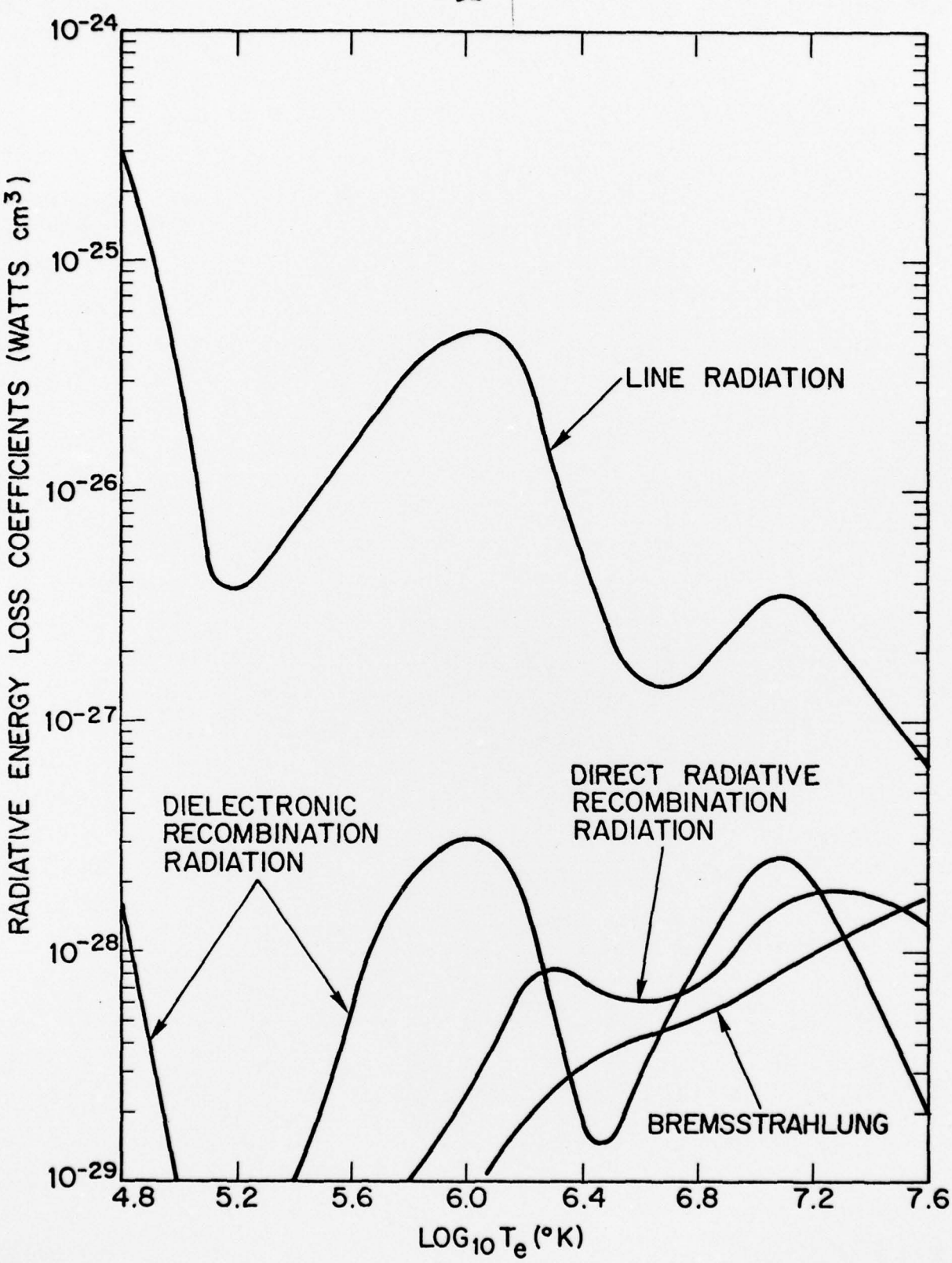
RADIATIVE ENERGY LOSS COEFFICIENTS (WATTS cm³)
10⁻²⁴
10⁻²⁵
10⁻²⁶
10⁻²⁷
10⁻²⁸
10⁻²⁹
LINE RADIATION
DIELECTRONIC RECOMBINATION RADIATION
DIRECT RADIATIVE RECOMBINATION RADIATION
BREMSSTRAHLUNG
4.8
5.2
5.6
6.0
6.4
6.8
7.2
7.6
LOG₁₀ Tₑ (°K)

Fig. 5